



· 论 著 ·

# 利用细胞膜片技术构建新型前列腺癌皮下移植瘤动物模型

周术奎<sup>1</sup>, 张东亮<sup>2</sup>, 王 翔<sup>2</sup>, 刘 磊<sup>1</sup>, 李 曾<sup>1</sup>, 杨盛柯<sup>1</sup>, 廖 洪<sup>1</sup>

1. 四川省肿瘤医院·研究所, 四川省癌症防治中心, 电子科技大学医学院泌尿外科, 四川 成都 610041;

2. 上海交通大学附属第一人民医院泌尿外科, 上海 200080

[摘要] 背景与目的: 传统前列腺癌皮下移植瘤模型的建立采取细胞悬液注射方式, 但该方式存在较大局限性。探索利用细胞膜片技术构建新型前列腺癌皮下移植瘤动物模型的可行性。方法: 将人前列腺癌细胞系DU145接种至35 mm温度敏感性细胞培养皿中, 连续培养制备前列腺癌细胞膜片, 并采用H-E染色和免疫组织化学方法鉴定。根据研究目的, 设置细胞悬液组和细胞膜片组, 细胞悬液组在BALB/c裸小鼠皮下注射DU145细胞悬液, 细胞膜片组在裸小鼠皮下注射DU145细胞膜片。移植后4周处死裸小鼠, 剥离两组移植瘤作进一步组织学分析, 包括胶原纤维含量、局部浸润及血管生成情况。同时, 解剖前列腺癌常见的转移脏器, 如骨、肺和肝脏等, 评估两组的全身转移情况。结果: 培养1周后可制备前列腺癌DU145细胞膜片, 大体观察呈现半透明胶质薄片, 具备较好的组织学强度。组织学染色见膜片状结构, 平均厚度约为(32.6±7.5) μm。DU145细胞标志物vimentin高表达, E-cadherin低表达, 胶原纤维含量丰富, 在膜片中高表达。皮下移植4周后, H-E染色显示, 细胞膜片组肿瘤结构致密, 有明显周围肌肉浸润, 而细胞悬液组肿瘤存在较多空泡, 与周围组织边界清楚。皮下移植4周后, 细胞膜片组移植瘤体积明显大于细胞悬液组, 两组测量肿瘤体积分别为(0.967±0.129)和(0.437±0.054) cm<sup>3</sup> ( $t=3.774$ ,  $P=0.0195$ )。马松染色显示, 细胞膜片组蓝色胶原纤维含量明显高于细胞悬液组, 两组吸光度( $D$ )值分别为0.023 0±0.001 1和0.014 0±0.000 7 ( $t=7.022$ ,  $P=0.0001$ )。CD31免疫组织化学染色表明, 在200倍显微镜视野下细胞膜片组和细胞悬液组移植瘤组织中微血管密度分别为53.20±3.56和32.40±4.98 ( $t=3.392$ ,  $P=0.0095$ )。皮下移植4周后, 两组通过大体解剖和H-E染色均未见到明显的全身转移病灶。结论: 利用细胞膜片技术构建前列腺癌皮下移植瘤动物模型具备可行性和一定优势, 与传统细胞悬液注射方式相比, 成瘤体积更大, 与周围组织浸润程度更深, 新生微血管密度更高, 胶原含量丰富, 更有助于揭示前列腺癌真实的生物学特征, 有望应用于前列腺癌分子遗传学研究、肿瘤耐药机制及新药研发等领域。

[关键词] 细胞膜片技术; 前列腺癌模型; 异位移植; 肿瘤微环境

DOI: 10.19401/j.cnki.1007-3639.2022.03.002

中图分类号: R737.25 文献标志码: A 文章编号: 1007-3639(2022)03-0200-07

**Developing a new animal model of subcutaneous transplanted prostate cancer with cell sheet technology** ZHOU Shukai<sup>1</sup>, ZHANG Dongliang<sup>2</sup>, WANG Xiang<sup>2</sup>, LIU Lei<sup>1</sup>, LI Zeng<sup>1</sup>, YANG Shengke<sup>1</sup>, LIAO Hong<sup>1</sup> (1. Department of Urology, Sichuan Cancer Hospital & Institute, Sichuan Cancer Center, School of Medicine, University of Electronic Science and Technology of China, Chengdu 610041, Sichuan Province, China; 2. Department of Urology, Shanghai General Hospital, Shanghai Jiao Tong University, Shanghai 200080, China)

Correspondence to: LIAO Hong E-mail: liaohong131@163.com

[Abstract] **Background and purpose:** Traditional preparation of subcutaneous transplanted tumor of prostate cancer relies on cell suspension injection. However, there are great limitations. The purpose of this study was to explore the feasibility of developing a new animal model of subcutaneous transplanted prostate cancer with cell sheet technology. **Methods:** Human prostate cancer DU145 cells were inoculated into a 35 mm temperature sensitive cell culture dish, and the prostate cancer cell sheet was prepared

基金项目: 四川省卫生和计划生育委员会重点研究项目(19ZD015)。

通信作者: 廖 洪 E-mail: liaohong131@163.com

by continuous culture and identified by H-E staining and immunohistochemistry. According to the research purpose, cell suspension group and cell membrane group were set up. DU145 cell suspension was subcutaneously injected into nude mice in cell suspension group, and DU145 cell sheet was subcutaneously injected into BALB/c nude mice in cell sheet group. The BALB/c nude mice were sacrificed 4 weeks after transplantation, and the grafted tumors in both groups were dissected for further histological analysis, including collagen fiber content, local infiltration and angiogenesis. Meanwhile, the common organs of prostate cancer metastasis, such as bone, lung and liver, were dissected to evaluate the systemic metastasis in both groups. **Results:** DU145 prostate cancer cell sheet could be prepared at 1 week after continuous culture. Histological staining revealed a membrane structure with an average thickness of  $(32.6 \pm 7.5) \mu\text{m}$ . The DU145 cell sheet was rich in collagen fibrin with high vimentin expression and low E-cadherin expression. H-E staining showed that the tumor structure was dense with obvious infiltration of surrounding muscles in the cell sheet group, while the tumor had more vacuoles and a clear boundary with surrounding tissues in the cell suspension group 4 weeks after subcutaneous transplantation. Moreover, the transplanted tumor volume was significantly higher in the cell sheet group than in the cell suspension group, and the measured tumor volume in the two groups were  $(0.967 \pm 0.129)$  and  $(0.437 \pm 0.054) \text{ cm}^3$  ( $t=3.774$ ,  $P=0.0195$ ), respectively. Masson staining showed that the content of blue collagen fiber was significantly higher in the cell sheet group than in the cell suspension group, and the optical densities ( $D$ ) value of the two groups were  $0.0230 \pm 0.0011$  and  $0.0140 \pm 0.0007$  ( $t=7.022$ ,  $P=0.0001$ ), respectively. Immunohistochemical staining of CD31 showed that the microvascular density per  $\times 200$  field in the cell sheet group and the cell suspension group were  $53.20 \pm 3.56$  and  $32.40 \pm 4.98$  ( $t=3.392$ ,  $P=0.0095$ ), respectively. Gross anatomy and H-E staining showed no obvious systemic metastasis in the two groups 4 weeks after subcutaneous transplantation. **Conclusion:** It is feasible and advantageous to develop the animal model of subcutaneous transplanted prostate cancer using cell sheet technology. Compared with traditional cell suspension injection method, the tumor volume was larger, the infiltration degree was deeper with surrounding tissues, the density of new microvessels was higher, and the collagen content was richer, which is more helpful to reveal the real biological characteristics of prostate cancer. It is expected to be applied in the research of molecular genetics of prostate cancer, drug resistance mechanism and drug discovery.

[ **Key words** ] Cell sheet technology; Prostate cancer model; Ectopic implantation; Tumor microenvironment

在全球范围内, 前列腺癌是男性第二大常见癌症, 占男性恶性肿瘤新发病例数的14.1%<sup>[1]</sup>。高收入国家的前列腺癌发病率和死亡率近年来处于下降或稳定状态, 但亚洲前列腺癌发病率快速上升<sup>[2]</sup>。2020年中国前列腺癌发病率约为15.6/10万人, 新发病例超11万, 死亡人数超5万<sup>[3]</sup>。晚期转移性前列腺癌经过18~24个月的内分泌治疗后最终发展成去势抵抗性前列腺癌<sup>[4]</sup>, 预后较差, 这与雄激素受体突变和相关信号转导通路密切相关, 但其机制仍不明确, 因此有必要探究前列腺癌的转移进展和耐药机制, 以便为晚期前列腺癌治疗确立新的靶向策略。肿瘤研究依赖于精确的动物模型。目前仍缺乏一种能够精准模拟体内真实环境的前列腺癌动物模型, 这也是导致转移性前列腺癌耐药和新药研发进展缓慢的重要原因之一。

近年来, Pang等<sup>[5]</sup>和Zhang等<sup>[6]</sup>利用细胞悬液注射方式构建前列腺癌皮下或原位移植瘤动物模型取得成功, 其操作简单、易学。然而, 这种方式存在细胞悬液渗漏、存活率低、成瘤率不

稳定、成瘤持续时间长等局限性, 容易引起移植瘤与原肿瘤内环境“失真”。细胞膜片技术是近年来发展起来的一种新型组织工程技术, 该技术无需胰酶消化和添加支架材料, 连续体外培养形成膜片状组织<sup>[7]</sup>。细胞膜片技术能够完整保留细胞外基质 (extracellular matrix, ECM), 保留细胞生长的微环境和生长因子, 其组织结构类似于天然组织<sup>[8]</sup>。因此, 细胞膜片技术已成为当前再生医学和组织工程领域的研究热点, 已被应用于泌尿系统修复重建, 包括膀胱<sup>[9]</sup>和尿道<sup>[10]</sup>。肿瘤细胞膜片是通过ECM黏附形成的, 可形成多层次结构, 而且具备一定力学强度, 使得肿瘤细胞膜片用于移植瘤成为可能<sup>[11-13]</sup>。目前国内外尚未见利用细胞膜片技术构建前列腺癌动物模型的相关研究报道, 本研究利用细胞膜片技术构建前列腺癌皮下移植瘤动物模型, 以细胞悬液注射作为参照组, 并采用组织学分析评估肿瘤形成效率, 以便为前列腺癌动物模型提供一种更优的选择。

## 1 材料和方法

### 1.1 实验动物与试剂

雄性BALB/c裸小鼠[6周龄, 体重20~25 g, 许可证号为SCXK(沪)2008-0016]购自上海西普尔-必凯实验动物有限公司; 饲养动物设施购自上海交通大学农生实验实习场有限公司; 实验动物保持在高效微粒空气过滤架的屏障设施中, 具有12 h暗光循环, 并允许自由获取食物和水。动物实验按照上海交通大学伦理委员会批准的实验程序进行。人前列腺癌细胞系DU145(HTB-81)购自美国模式培养物保藏所(American Type Culture Collection, ATCC); 0.25%胰酶、胎牛血清(fetal bovine serum, FBS)、RPMI-1640培养基和双抗等均购自美国Gibco公司; 35 mm温度敏感性细胞培养皿购自美国Thermo Fisher Scientific公司; 细胞培养耗材购自美国Corning公司; 4, 6-二氨基-2-苯基吲哚(4, 6-diamino-2-phenyl indole, DAPI)和鼠尾胶原蛋白I型购自美国Sigma公司; 马松三色染色试剂盒购自北京索莱宝科技有限公司; 兔抗小鼠单克隆E-cadherin、vimentin、CD31和I型胶原抗体均购自美国Abcam公司。

### 1.2 前列腺癌DU145细胞膜片培养

人前列腺癌细胞系DU145复苏后, 重悬在含10%FBS、100 U/mL青霉素和100 μg/mL链霉素的RPMI-1640培养基中, 置于37 °C、CO<sub>2</sub>体积分数为5%的培养箱内继续培养, 每2~3 d更换1次培养基。为促进细胞黏附和细胞膜片形成, 预先以500 μg/mL鼠尾胶原蛋白I型包被35 mm温度敏感性细胞培养皿, 在4 °C的避风条件下保存过夜。当培养DU145细胞达到95%融合时, 用0.5%胰酶消化, 1 000 r/min离心5 min(离心半径为15 cm), 细胞重悬, 计数后接种至包被培养皿中连续培养, 每2 d换液1次, 连续培养7 d即可成膜, 于20 °C培养15 min预冷后可收获完整前列腺癌DU145细胞膜片。

### 1.3 前列腺癌DU145细胞膜片鉴定

前列腺癌DU145细胞膜片用4%多聚甲醛

溶液固定, 石蜡包埋, 切片5 μm, 行H-E染色。同时, 采用免疫组织化学染色观察细胞膜片特异性蛋白E-cadherin、vimentin和胶原纤维, 0.5%Triton-X100破膜, 1%牛血清白蛋白(bovine serum albumin, BSA)常温封闭切片30 min, 然后分别用E-cadherin(1:500)、vimentin(1:500)和I型胶原免疫球蛋白G(immunoglobulin G, IgG)兔抗小鼠抗体(1:500)温育, 4 °C处理过夜。用磷酸缓冲盐溶液(phosphate-buffered saline, PBS)洗涤后, 将切片与辣根过氧化物酶(horse radish peroxidase, HRP)标记山羊抗兔IgG抗体(1:1 000)室温温育1 h, 二氨基联苯胺(diaminobenzidine, DAB)染色, 苏木精复染, 在正置显微镜下观察。

### 1.4 细胞膜片皮下移植成瘤

将6只雄性BALB/c裸小鼠随机分为2组, 每组3只, 分为细胞悬液组和细胞膜片组。预先以0.5%胰酶消化单张细胞膜片, 1 000 r/min离心5 min(离心半径为15 cm), 重悬后计数单张膜片细胞数量, 约 $2 \times 10^6$ 个。对于细胞膜片组, 将单张细胞膜片与培养液混合, 体积100 μL, 注射于裸小鼠左背部近前肢皮下组织, 注射后轻压注射点约30 s。对于细胞悬液组, 当培养DU145细胞达到95%融合时, 0.5%胰酶消化, 1 000 r/min离心5 min(离心半径为15 cm), Matrigel基质胶细胞重悬后计数, 随后将与单张细胞膜片细胞数目相等的细胞悬液100 μL注射于裸小鼠左背部近前肢皮下组织, 注射后轻压注射点约30 s。

### 1.5 皮下移植瘤测量

从移植1周起, 每3 d观察两组裸小鼠生存及皮下移植瘤的情况, 移植4周后处死实验动物, 剥离皮下移植瘤, 连带部分周围组织, 并用标尺测量移植瘤的最大直径( $a$ )和最小直径( $b$ ), 肿瘤体积计算公式<sup>[14]</sup>:  $V = a \times b^2 \times \pi / 6$ 。

### 1.6 体内移植瘤的组织学分析

用4%多聚甲醛溶液固定移植瘤, 石蜡包埋, 切片5 μm, 行H-E染色。采用免疫组织化学染色观察血管标志物CD31的表达情况, 0.5%Triton-X100破膜, 1%BSA常温封闭切片30 min, 然后分别用CD31兔抗小鼠抗体

(1:500)温育,4℃处理过夜。用PBS洗涤后,将切片与HRP标记山羊抗兔IgG抗体(1:1000)室温温育,DAB染色,苏木精复染,在正置显微镜下观察。同时,根据说明书流程,利用马松三色染色试剂盒观察移植瘤中的胶原蛋白表达情况,其中胶原纤维组织呈蓝色。

### 1.7 全身转移情况观察

皮下注射移植4周后,处理裸小鼠,解剖前列腺癌常见的转移脏器,如移植附近前肢骨、肺和肝脏,大体观察上述脏器有无结节,并进行H-E染色,评估两组在骨、肺和肝脏等全身重要脏器的转移情况。

### 1.8 统计学处理

应用SPSS 19.0统计学软件对数据进行分析,定量资料以 $\bar{x} \pm s$ 表示,组间定量资料比较采用 $t$ 检验,

$P < 0.05$ 为差异有统计学意义。

## 2 结果

### 2.1 前列腺癌DU145细胞膜片体外培养与鉴定

前列腺癌DU145细胞呈多角形或梭形,大小不一,形态不规则,细胞轮廓清晰。连续培养7 d即可成膜,在光镜下可见细胞膜片表面大量白色絮状ECM分布,细胞紧密连接,细胞间边界不清。降低培养温度后,可完整剥离前列腺癌DU145细胞膜片,大体观察呈现半透明胶质薄片,表面平滑,质地均匀。H-E染色显示,细胞膜片由3~5层细胞组成,厚度为 $(32.6 \pm 7.5) \mu\text{m}$  ( $n=3$ ),vimentin和I型胶原经免疫组织化学染色呈强阳性,而E-cadherin染色呈阴性(图1)。

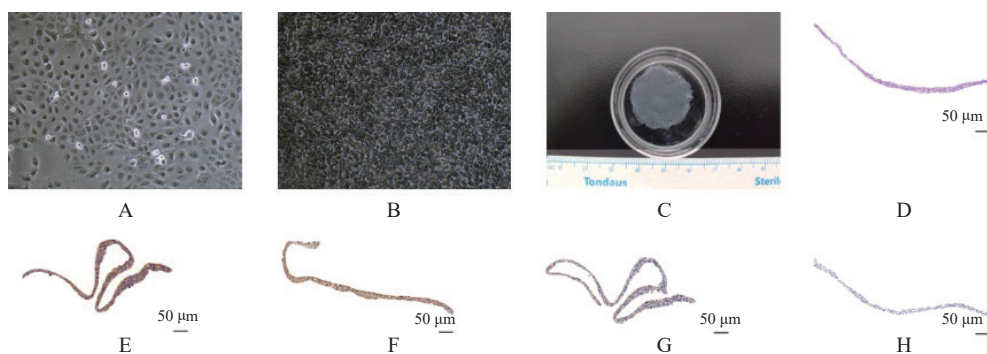


图1 DU145细胞膜片培养与鉴定

Fig. 1 Culture and identification of DU145 cell sheet

A: DU145 cell culture, cell fusion degree was 90%; B: DU145 cell sheet was observed under the light microscope; C: general view of DU145 cell sheet formation; D: DU145 cells were observed by H-E staining; E: Strong positive expression of vimentin immunohistochemical staining; F: Strong positive expression of type I collagen immunohistochemical staining; G: Negative expression of E-cadherin immunohistochemical staining; H: Negative control.

### 2.2 细胞膜片皮下移植成瘤与大体观察

两组裸小鼠皮下移植后均生存良好,两组成瘤率均为100% (3/3),均表现为类椭圆形实质性肿块,移植4周后处死裸小鼠并剥离肿瘤,其中细胞膜片组移植瘤边界不清,不易与周围组织完整剥离。细胞悬液组移植瘤包膜较完整,易剥离。大体观察显示,细胞膜片组移植瘤体积明显高于细胞悬液组,两组测量肿瘤体积分别为 $(0.967 \pm 0.129)$ 和 $(0.437 \pm 0.054) \text{cm}^3$  ( $t=3.774, P=0.0195$ ,图2)。

### 2.3 体内移植瘤的组织学分析

注射4周后,H-E染色可见细胞膜片组肿瘤

细胞生长密集,细胞间连接紧密,较少空泡形成,且肿瘤细胞浸润性生长至临近肌肉组织内,组织间分界欠清,而细胞悬液组细胞与细胞间连接普遍松散,肿瘤组织内见明显空泡形成和多发透明样改变,部分融合呈液化坏死,且与临近肌肉组织分界清楚。马松染色显示,细胞膜片组蓝色胶原纤维含量明显高于细胞悬液组,两组光密度值分别为 $0.0230 \pm 0.0011$ 和 $0.0140 \pm 0.0007$  ( $t=7.022, P=0.0001$ )。CD31免疫组织化学染色表明,在200倍显微镜视野下细胞膜片组和细胞悬液组移植瘤组织中微血管密度(microvascular density, MVD)分别为 $53.20 \pm 3.56$ 和 $32.40 \pm 4.98$

( $t=3.392$ ,  $P=0.0095$ , 图3)。

### 2.4 全身主要器官的转移情况检测

注射4周后, 对全身前列腺癌常见的转移脏

器(如骨、肺和肝脏等)进行大体解剖, 肉眼观察未见明显结节或肿块。H-E染色显示, 两组的骨、肺和肝脏均未见明显转移病灶(图4)。

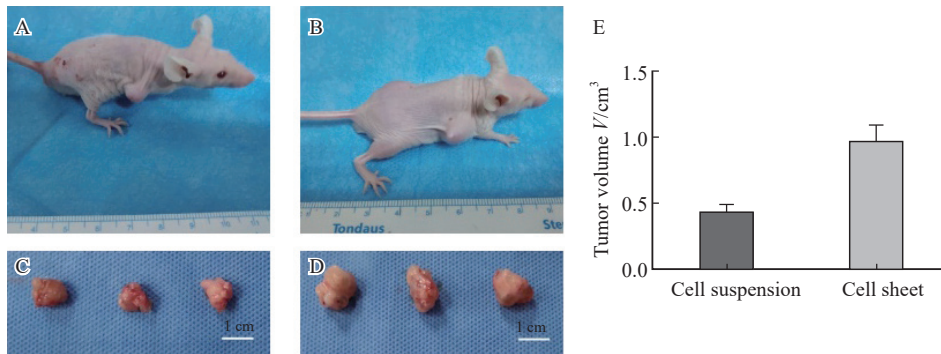


图2 细胞膜片皮下移植成瘤与大体观察

Fig. 2 Subcutaneous transplantation tumor formation of cell sheet and gross observation

A: The appearance of nude mice in cell suspension group after 4 weeks transplantation; B: The appearance of nude mice in cell sheet group after 4 weeks transplantation; C: Exfoliated transplantation tumor in cell suspension group; D: Exfoliated transplantation tumor in cell sheet group; E:  $P<0.05$ , comparison of transplantation tumor volume between the two groups.

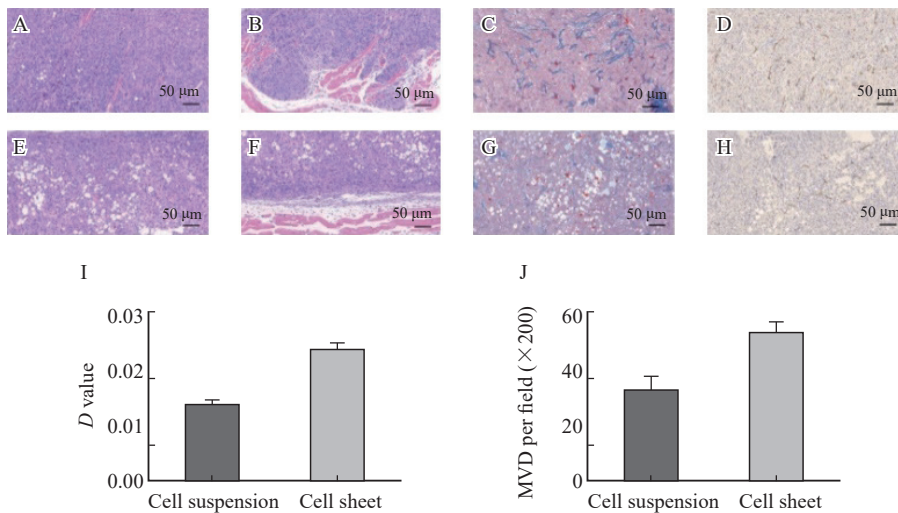


图3 体内移植瘤组织学分析

Fig. 3 Histological analysis of transplanted tumor in vivo

A: H-E staining in cell sheet group; B: Tumor boundary with H-E staining in cell sheet group; C: Masson staining of cell sheet group; D: CD31 immunohistochemical staining in cell sheet group; E: H-E staining in cell suspension group; F: Tumor boundaries with H-E staining in cell suspension group; G: Masson staining in cell suspension group; H: CD31 immunohistochemical staining in cell suspension group; I:  $P<0.05$ , comparison of optical density of masson staining between the two groups; J:  $P<0.05$ , comparison of MVD between the two groups.

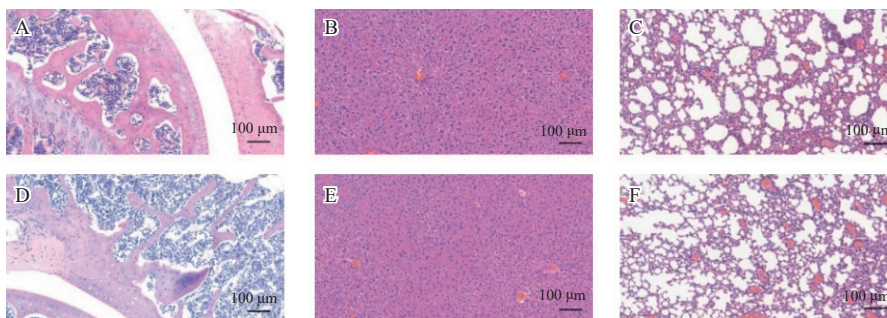


图4 全身主要器官转移情况H-E染色

Fig. 4 H-E staining of major organs in the whole body

A: The anterior limb bone in cell sheet group; B: The lung in cell sheet group; C: The liver in cell sheet group; D: The anterior limb bone in cell suspension group; E: The lung in cell suspension group; F: The liver in cell suspension group.

### 3 讨 论

利用体外培养前列腺癌细胞及其相关细胞注射方式构建前列腺癌皮下移植瘤动物模型一直是初步检测肿瘤基因表型、研发抗肿瘤药物及识别肿瘤标志物的主要方式,但这两种肿瘤研究方式存在较大缺陷且难以克服,前者缺乏体内环境,后者难以模拟真实的肿瘤生物学行为。肿瘤细胞、ECM及多种细胞因子是肿瘤微环境的主要组成部分<sup>[15]</sup>。前列腺癌细胞贴壁生长,需要酶消化来获取肿瘤细胞悬液,这种方式会损失相当数量的细胞,并破坏ECM成分,会不可避免地影响肿瘤细胞活性和信号转导通路,继而改变肿瘤细胞基因和蛋白的表达和表型特征,导致实验室肿瘤研究结果在向临床转化应用时困难重重。

DU145细胞系是首个前列腺癌细胞系,于1975年分离自前列腺癌患者的脑转移病灶,为雄激素非依赖性前列腺癌细胞<sup>[16]</sup>。本研究免疫组织化学染色提示vimentin高表达,E-cadherin低表达,符合DU145细胞标志蛋白特征。本研究发现,在温度敏感性细胞培养皿中预先包被鼠尾胶原蛋白I型对于DU145细胞膜片的形成至关重要,否则DU145细胞在连续培养过程中会坏死脱落,形成的是细胞簇而非细胞膜片。前列腺癌属于惰性肿瘤,具有细胞增殖能力相对较弱、生长速度慢和难以成瘤的特点。我们推测,与成纤维细胞<sup>[17]</sup>或间充质干细胞<sup>[18]</sup>等高成膜率细胞类型相比,DU145细胞的黏附和扩散能力较差,胶原分泌不足,因此需要预先包被胶原蛋白促进其黏附生长。另外,传统细胞悬液体内注射后,细胞固定效果较差,常会出现细胞渗漏,继而播散转移。为克服这一局限性,Pavlou等<sup>[19]</sup>使用Matrigel基质胶混合肿瘤细胞进行局部注射,增加细胞间黏附,以加速肿瘤形成。然而,外源性Matrigel基质胶使用的同时也会增加注射部位免疫和炎症反应<sup>[20]</sup>。本研究的细胞膜片中含丰富ECM,细胞间紧密连接,注射后很少发生迁移和细胞渗漏,最大化地满足肿瘤原位注射的要求。同时,这种天然ECM连接而成的细胞膜片移植后

能避免免疫和炎症反应,且不会引起组织塌陷。

肿瘤微环境中的基质细胞通过分泌可溶性分子或外泌体来促进肿瘤细胞的生长和转移。ECM中的胶原蛋白和纤连蛋白为肿瘤细胞提供物理支持,同时也充当可溶性因子和外泌体的结合支架<sup>[21]</sup>。血管生成是肿瘤生长的必要条件,肿瘤组织内MVD越高,则越有助于肿瘤获得足够的营养和排出代谢废物,故抗血管生成药物在实体瘤的治疗中占据重要地位。早前研究<sup>[22]</sup>表明,血管化缺失会限制实体瘤生长,在无血管角膜中,肿瘤生长缓慢且呈线性,但血管化后生长迅速且呈指数增长。ECM和活性因子参与肿瘤诱导的血管生成、血管稳定和维持血管内皮细胞生存<sup>[23]</sup>。在本研究中,两组的成瘤率均达到100%,但细胞膜片组肿瘤组织内MVD明显高于细胞悬液组,且胶原纤维含量丰富,能为细胞膜片中保留ECM和活性因子,促进血管再生。同时,与细胞悬液组相比,细胞膜片组肿瘤从宿主组织中获得了充足氧气和营养物质,成瘤时间缩短,细胞紧密连接,空洞较少,肿瘤浸润周围结缔肌肉组织,并向组织内新形成的血管扩张。

然而,本研究也存在一些局限性:首先,每组裸小鼠数量太少,可能导致统计误差和真实世界偏倚;其次,出于动物伦理保护目的,本研究规定全部裸小鼠移植瘤生长最大直径不超过2 cm,而前列腺癌是一种惰性肿瘤,局部生长和侵袭性转移进展均较缓慢,细胞移植后观察时间不够长,注射4周后对裸小鼠骨、肺和肝脏等前列腺癌常见的转移脏器进行相关离体检测,未观察到明显的脏器转移现象,如后续构建转移性前列腺癌细胞膜片动物模型,需加大初始移植细胞数量或延长移植瘤观察时间;最后,本研究主要比较两种方法体内成瘤后在大体方面的差异,如体积、H-E染色、胶原含量及血管形成等,没有深入解析分子生物学机制,有待后续研究进一步全面分析两种方法构建前列腺癌皮下移植瘤模型的差异。

#### [参 考 文 献]

[1] SUNG H, FERLAY J, SIEGEL R L, et al. Global cancer

- statistics 2020: GLOBOCAN estimates of incidence and mortality worldwide for 36 cancers in 185 countries [J]. *CA Cancer J Clin*, 2021, 71(3): 209–249.
- [ 2 ] CULP M B, SOERJOMATARAM I, EFSTATHIOU J A, et al. Recent global patterns in prostate cancer incidence and mortality rates [J]. *Eur Urol*, 2020, 77(1): 38–52.
- [ 3 ] 中国抗癌协会泌尿男生殖系统肿瘤专业委员会前列腺癌学组. 前列腺癌筛查中国专家共识 (2021年版) [J]. *中国癌症杂志*, 2021, 31(5): 435–440.  
Prostate Cancer Group, Urogenital Tumor Professional Committee, Chinese Anti-cancer Association. Chinese expert consensus on prostate cancer screening (2021 version) [J]. *China Oncol*, 2021, 31(5): 435–440.
- [ 4 ] MOLLICA V, RIZZO A, ROSELLINI M, et al. Bone targeting agents in patients with metastatic prostate cancer: State of the art [J]. *Cancers (Basel)*, 2021, 13(3): 546.
- [ 5 ] PANG K, XIE C Y, YANG Z R, et al. Monitoring circulating prostate cancer cells by *in vivo* flow cytometry assesses androgen deprivation therapy on metastasis [J]. *Cytometry A*, 2018, 93(5): 517–524.
- [ 6 ] ZHANG Y, TONERI M, MA H Y, et al. Real-time GFP intravital imaging of the differences in cellular and angiogenic behavior of subcutaneous and orthotopic nude-mouse models of human PC-3 prostate cancer [J]. *J Cell Biochem*, 2016, 117(11): 2546–2551.
- [ 7 ] IMASHIRO C, SHIMIZU T. Fundamental technologies and recent advances of cell-sheet-based tissue engineering [J]. *Int J Mol Sci*, 2021, 22(1): E425.
- [ 8 ] THUMMARATI P, KINO-OKA M. Effect of co-culturing fibroblasts in human skeletal muscle cell sheet on angiogenic cytokine balance and angiogenesis [J]. *Front Bioeng Biotechnol*, 2020, 8: 578140.
- [ 9 ] WANG Y, ZHOU S K, YANG R X, et al. Bioengineered bladder patches constructed from multilayered adipose-derived stem cell sheets for bladder regeneration [J]. *Acta Biomater*, 2019, 85: 131–141.
- [ 10 ] ZHOU S K, YANG R X, ZOU Q S, et al. Fabrication of tissue-engineered bionic urethra using cell sheet technology and labeling by ultrasmall superparamagnetic iron oxide for full-thickness urethral reconstruction [J]. *Theranostics*, 2017, 7(9): 2509–2523.
- [ 11 ] AKIMOTO J, NAKAYAMA M, TAKAGI S, et al. Efficient intrahepatic tumor generation by cell sheet transplantation to fabricate orthotopic hepatocarcinoma-bearing model mice for drug testing [J]. *J Biomed Mater Res A*, 2019, 107(5): 1071–1079.
- [ 12 ] ALSHAREEDA A T, ALSOWAYAN B, ALMUBARAK A, et al. Exploring the potential of mesenchymal stem cell sheet on the development of hepatocellular carcinoma *in vivo* [J]. *J Vis Exp*, 2018, (139): 57805.
- [ 13 ] AKIMOTO J, NAKAYAMA M, TAKAGI S, et al. Improved *in vivo* subcutaneous tumor generation by cancer cell sheet transplantation [J]. *Anticancer Res*, 2018, 38(2): 671–676.
- [ 14 ] BAL E, PARK H S, BELAID-CHOUCAIR Z, et al. Mutations in ACTR1 and its enhancer RNA elements lead to aberrant activation of Hedgehog signaling in inherited and sporadic basal cell carcinomas [J]. *Nat Med*, 2017, 23(10): 1226–1233.
- [ 15 ] LÓPEZ DE ANDRÉS J, GRIÑÁN-LISÓN C, JIMÉNEZ G, et al. Cancer stem cell secretome in the tumor microenvironment: a key point for an effective personalized cancer treatment [J]. *J Hematol Oncol*, 2020, 13(1): 136.
- [ 16 ] NAMEKAWA T, IKEDA K, HORIE-INOUE K, et al. Application of prostate cancer models for preclinical study: advantages and limitations of cell lines, patient-derived xenografts, and three-dimensional culture of patient-derived cells [J]. *Cells*, 2019, 8(1): E74.
- [ 17 ] SAKAI Y, YAMANOCHI K, OHASHI K, et al. Vascularized subcutaneous human liver tissue from engineered hepatocyte/fibroblast sheets in mice [J]. *Biomaterials*, 2015, 65: 66–75.
- [ 18 ] WANG Z F, HAN L, SUN T Y, et al. Osteogenic and angiogenic lineage differentiated adipose-derived stem cells for bone regeneration of calvarial defects in rabbits [J]. *J Biomed Mater Res A*, 2021, 109(4): 538–550.
- [ 19 ] PAVLOU M, SHAH M, GIKAS P, et al. Osteomimetic matrix components alter cell migration and drug response in a 3D tumour-engineered osteosarcoma model [J]. *Acta Biomater*, 2019, 96: 247–257.
- [ 20 ] WU H W, HE Z X, LI X N, et al. Efficient and consistent orthotopic osteosarcoma model by cell sheet transplantation in the nude mice for drug testing [J]. *Front Bioeng Biotechnol*, 2021, 9: 690409.
- [ 21 ] CHENG Y Q, WANG S B, LIU J H, et al. Modifying the tumour microenvironment and reverting tumour cells: new strategies for treating malignant tumours [J]. *Cell Prolif*, 2020, 53(8): e12865.
- [ 22 ] RIBATTI D, PEZZELLA F. Overview on the different patterns of tumor vascularization [J]. *Cells*, 2021, 10(3): 639.
- [ 23 ] DE PALMA M, BIZIATO D, PETROVA T V. Microenvironmental regulation of tumour angiogenesis [J]. *Nat Rev Cancer*, 2017, 17(8): 457–474.

(收稿日期: 2021-12-28 修回日期: 2022-02-19)